Cyclic Voltammetry

Bing Joe Hwang

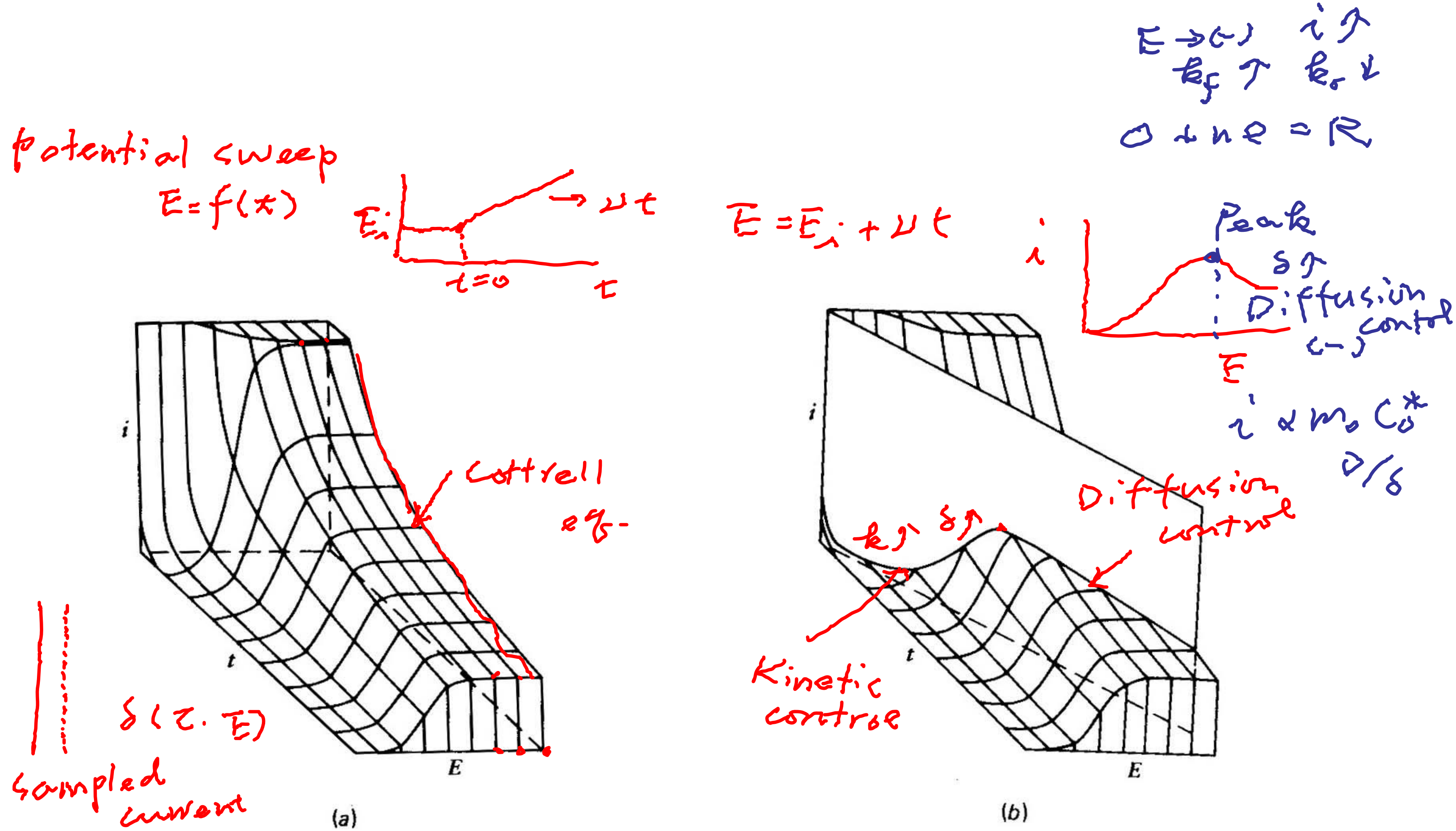

Figure 6.1.1

(*a*) Representation of a portion of the *i*-*t*-*E* surface for a nernstian reaction. Potential axis is in units of 60/*n* mV. (*b*) Linear potential sweep across this surface. [Reprinted with permission from W. H. Reinmuth, *Anal. Chem.*, **32**, 1509 (1960). Copyright 1960, American Chemical Society.]

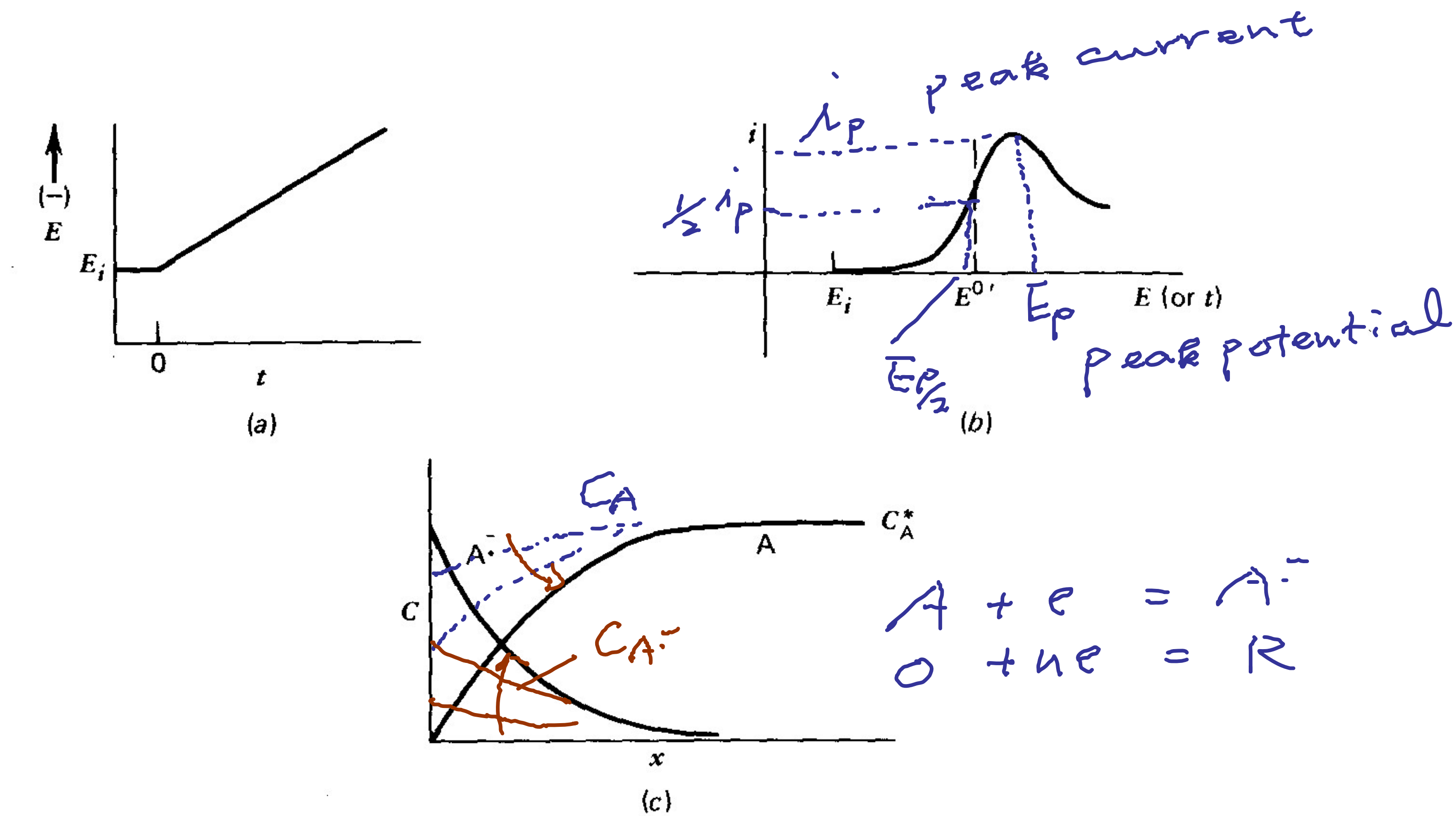

Figure 6.1.2

(*a*) Linear potential sweep or ramp starting at E_i. (*b*) Resulting *i-E* curve. (*c*) Concentration profiles of A and $A^{\overline{\cdot}}$ for potentials beyond E_p.

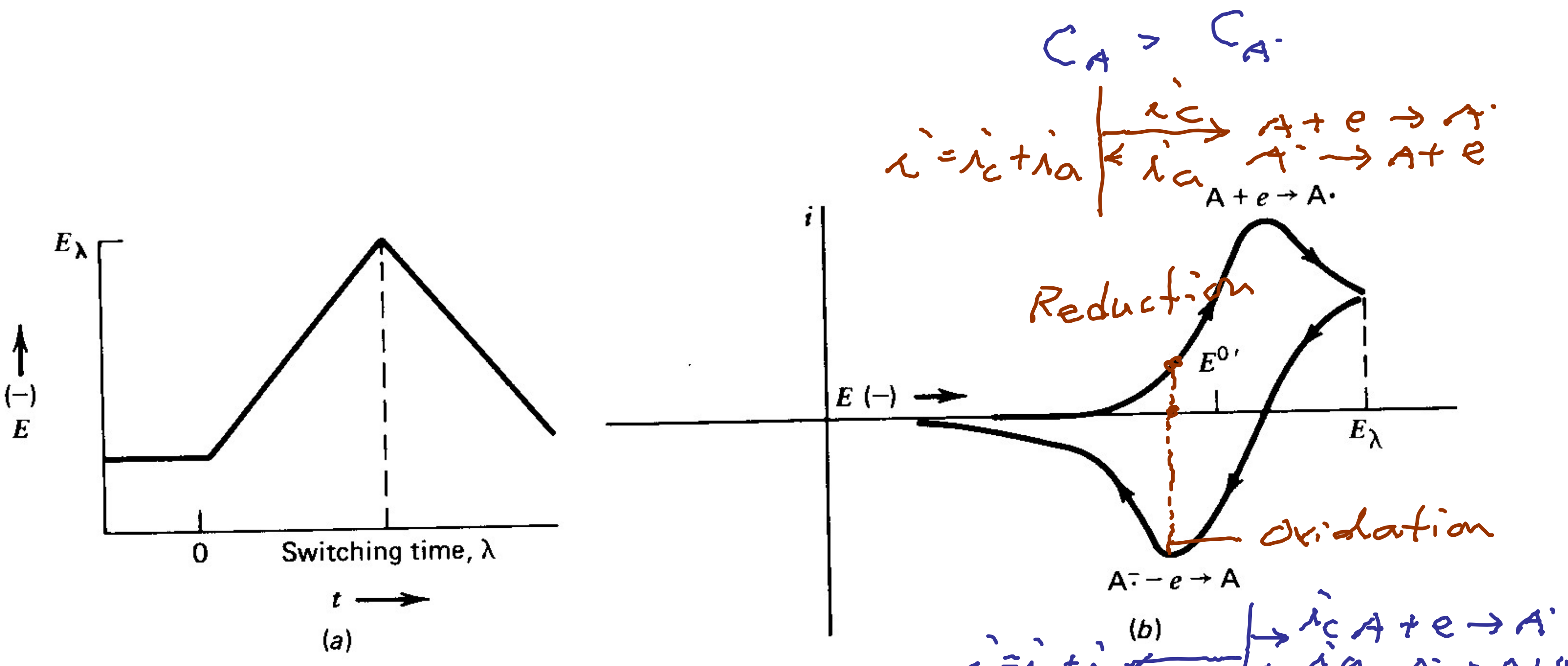

Figure 6.1.3

(*a*) Cyclic potential sweep. (*b*) Resulting cyclic voltammogram.

6.2 Nernstian rxn

$$E = E_i - \nu t$$

ν ↑ sweep rate, scan rate — V/s, mV/s

B.C. 2

$$\frac{C_O(0,t)}{C_R(0,t)} = \exp\left[\frac{nF}{RT}\left(E - E^{0'}\right)\right]$$

$$= \exp\left[\frac{nF}{RT}\left(E_i - \nu t - E^{0'}\right)\right]$$

$$= \theta \exp\left(-\frac{nF}{RT}\nu t\right) = \theta e^{-\sigma t}$$

θ = $\exp\left(\frac{nF}{RT}(E_i - E^{0'})\right)$

$$\sigma = \frac{nF}{RT}\nu$$

$$i = nFAC_O^*(\pi D_O \sigma)^{1/2} \chi(\sigma t)$$

Table 6.2.1 → $\chi(\sigma t)$

$$i = nFAC_O^*(\pi D_O \sigma)^{1/2}\,\chi(\sigma t)$$

$$i_p = nFAC_O^*(D_O \sigma)^{1/2} \cdot 0.4463 \qquad 6.2.18$$

$\frac{n(E-E_{1/2})}{RT/F}$	$n(E-E_{1/2})$ mV at 25°C	$\pi^{1/2}\chi(\sigma t)$ (planar)	$\phi(\sigma t)$ (spherical)
⋮	4?	0.09	
⋮	120	⋮	
⋮	100	⋮	
	⋮		
	40	0.16	
	−28.5 (peak potential)	peak 0.445 ⟵ 0.4463* 0.446	0.7516

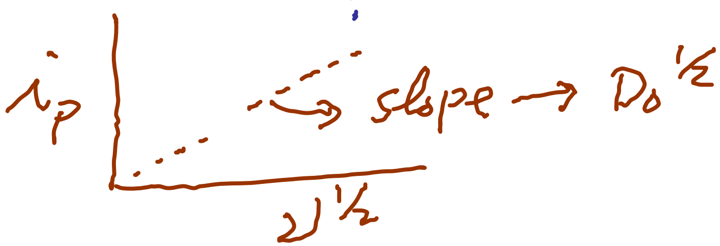

$$i_p = 0.4463 \cdot \left(\frac{F^3}{RT}\right)^{1/2} n^{3/2} A D_O^{1/2} C_O^* \nu^{1/2}$$

$$E_p - E_{1/2} = \pm \frac{28.5}{n} \text{ mV at } 25^\circ C \quad \begin{cases} - & \text{cathodic scan} \\ + & \text{Anodic scan} \end{cases}$$

$$E_{p/2} - E_{1/2} = \frac{28.0}{n} \text{ mV at } 25^\circ C$$

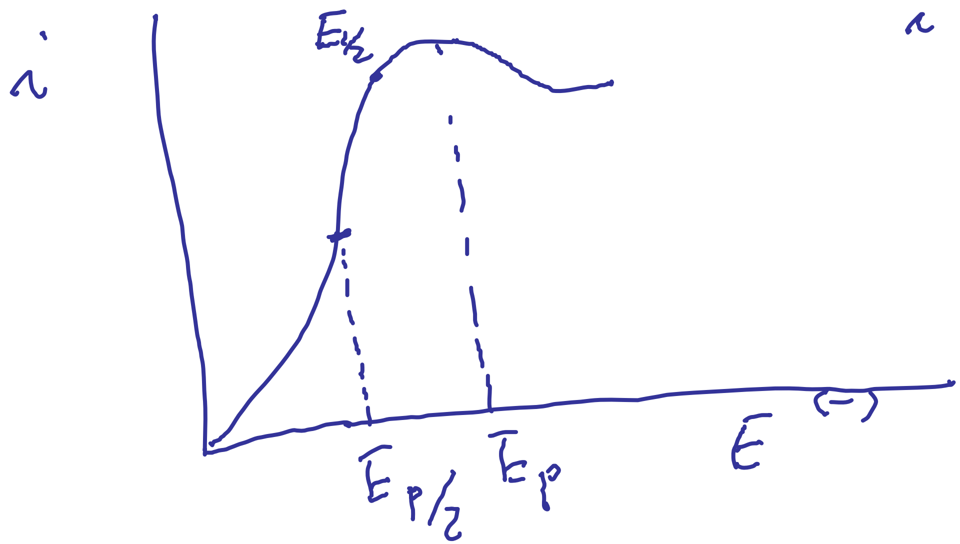

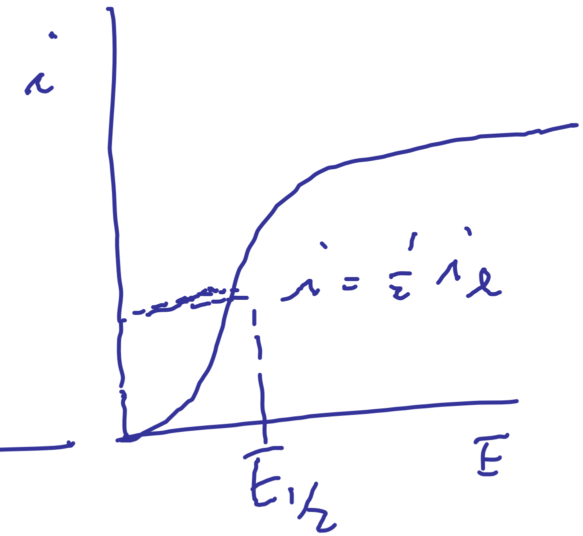

$$|E_p - E_{p/2}| = \frac{56.5}{n} \text{ mV at } 25^\circ C$$

6.2.3 Spherical electrodes & UMEs

UMEs

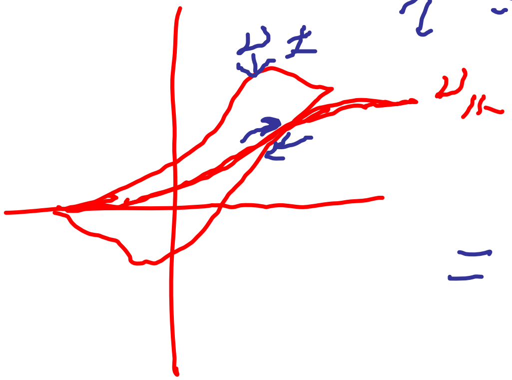

$$i = i(\text{plane}) + \frac{nFAD_0 C_0^* \phi(\sigma t)}{r_0}$$

$$= nFAC_0^*(\pi D_0 \sigma)^{1/2} \chi(\sigma t) + \frac{\quad\quad\quad}{r_0}$$

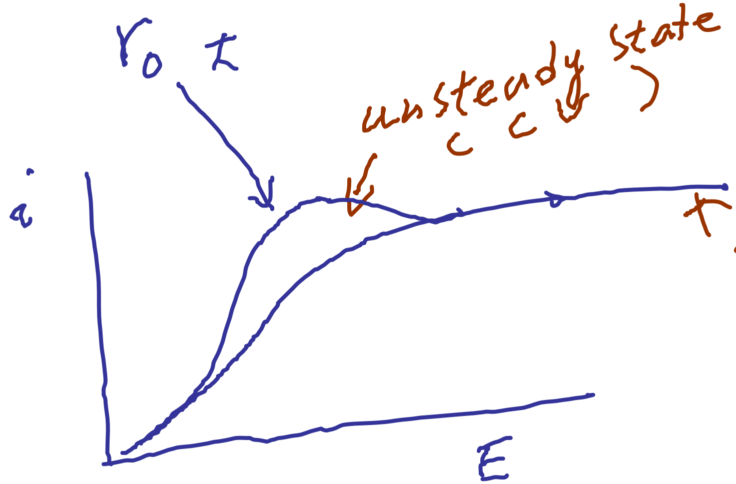

unsteady state (c ↓)

r_0 ↑ ν 小

steady state

$\nu << RTD/nFr_0^2$

6.2 Nernstian Systems

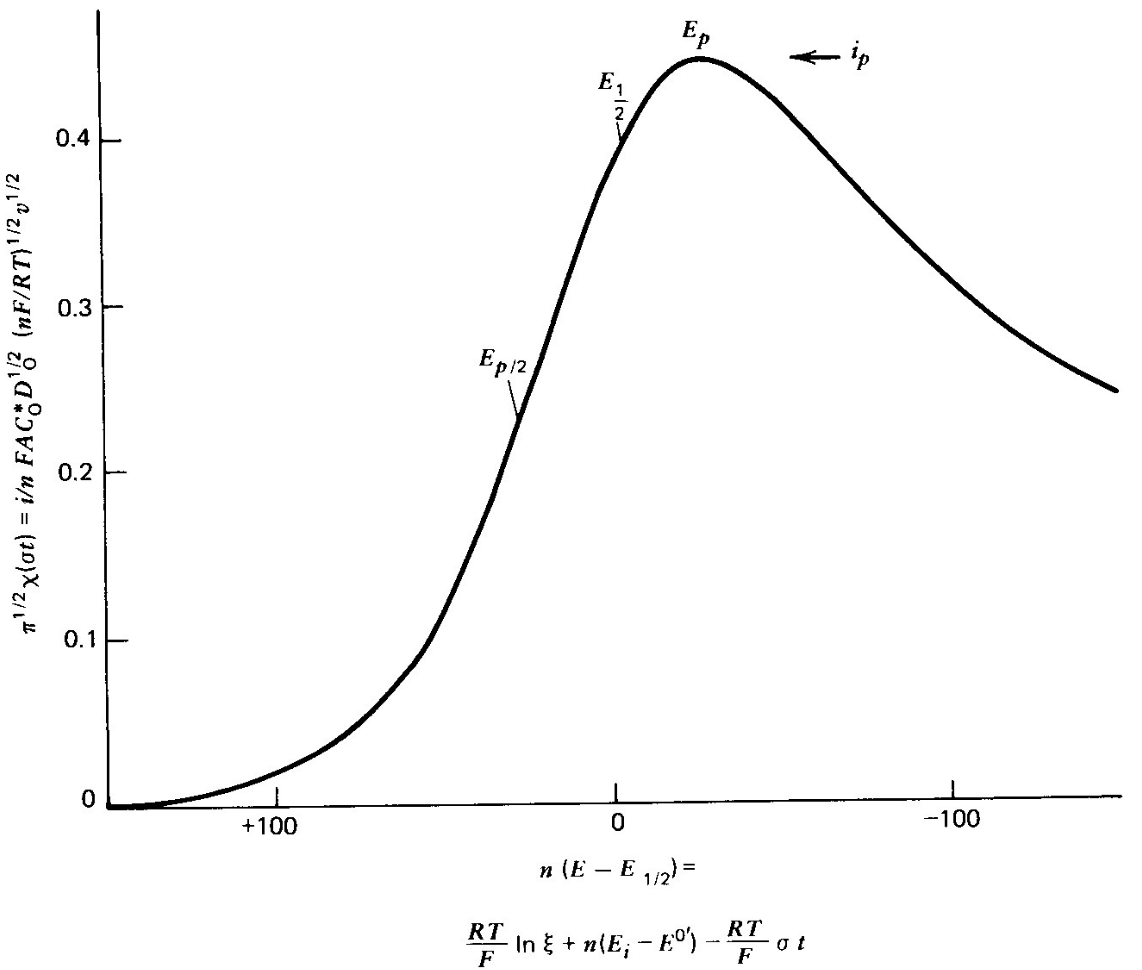

Figure 6.2.1
Linear potential sweep voltammogram in terms of dimensionless current function.

Table 6.2.1

Current Functions $\sqrt{\pi}\chi(\sigma t)$ for Reversible Charge Transfer (3)[a]

$(E - E_{1/2})n$[b] mV	$\sqrt{\pi}\chi(\sigma t)$	$\phi(\sigma t)$	$(E - E_{1/2})n$[b] mV	$\sqrt{\pi}\chi(\sigma t)$	$\phi(\sigma t)$
120	0.009	0.008	−5	0.400	0.548
100	0.020	0.019	−10	0.418	0.596
80	0.042	0.041	−15	0.432	0.641
60	0.084	0.087	−20	0.441	0.685
50	0.117	0.124	−25	0.445	0.725
45	0.138	0.146	−28.50	0.4463	0.7516
40	0.160	0.173	−30	0.446	0.763
35	0.185	0.208	−35	0.443	0.796
30	0.211	0.236	−40	0.438	0.826
25	0.240	0.273	−50	0.421	0.875
20	0.269	0.314	−60	0.399	0.912
15	0.298	0.357	−80	0.353	0.957
10	0.328	0.403	−100	0.312	0.980
5	0.355	0.451	−120	0.280	0.991
0	0.380	0.499	−150	0.245	0.997

[a] To calculate the current:

1. $i = i(\text{plane}) + i(\text{spherical correction})$.
2. $i = nFA\sqrt{\sigma D_O}C_O^*\sqrt{\pi}\chi(\sigma t) + nFAD_OC_O^*(1/r_0)\phi(\sigma t)$.
3. $i = 602\, n^{3/2}A\sqrt{D_O v}C_O^*[\sqrt{\pi}\chi(\sigma t) + 0.160(\sqrt{D_O}/r_0\sqrt{nv})\phi(\sigma t)]$ amperes at 25°. Units for step 3 are: A, cm^2; D_O, cm^2/sec; v, V/sec; C_O^*, moles/liter; r_0, cm.

[b] $E_{1/2} = E^{0\prime} + (RT/nF)\ln(D_R/D_O)^{1/2}$

For reversible redox couples

1. $i_p = 0.4463nFAC_O^*(nF/RT)^{1/2}v^{1/2}D_O^{1/2}$

$= 2.69 \times 10^5\ n^{3/2}\ A\ D_O^{1/2}v^{1/2}C_O^*$

2. $E_p - E_{p/2} = 2.2\ (RT/nF) = 56.6/n$ mV at 25°C

3. $E_p = E_{O/R}^{o'} - 0.028.5/n$ V (independent of v)

4. $i_p = i_{p'} - i_{background}$; $i_{p'}$: measured peak current

• Double-layer Capacitance

$C_d = \frac{Q}{V}$; $Q = C_d \cdot V$

$\frac{dQ}{dt} = C_d \frac{dV}{dt} = -\nu C_d$

$|i_c| = A \cdot C_d \cdot \nu$

$\frac{N}{S} \sim \frac{|i_c|}{i_p} = \frac{C_d \nu^{1/2} \cdot 10^{-5}}{2.69 n^{3/2} D_0^{1/2} C_0^*}$

$\frac{S}{N} \propto \frac{1}{\nu^{1/2}} \cdot C_0^*$

$i_p \propto \nu^{1/2}$

$E = E_i - \nu t$

$\frac{dE}{dt} = -\nu$

• IR drop effect

iR_u

$E = E_{applied} + iR_u$

$-500 \quad -600 \quad +100$

⇒ IR compensation

• Time const.

$R_u C_d \Rightarrow 1\,ms$

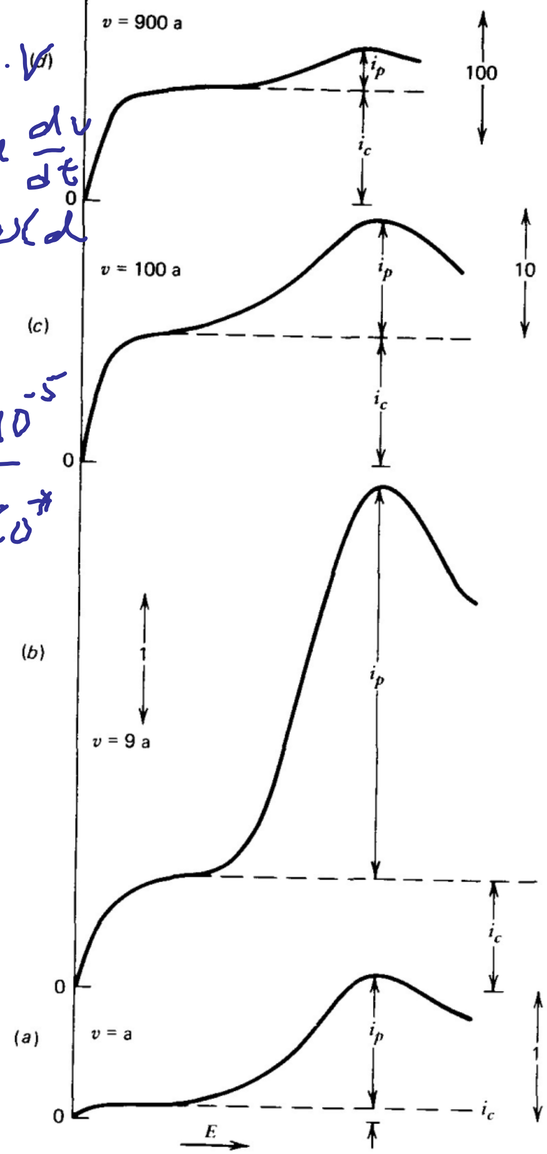

Figure 6.2.2
Effect of double-layer charging at different sweep rates on linear potential sweep voltammogram. Curves are plotted with the assumption that C_d is independent of E. The magnitude of the charging current, i_c, and the faradaic peak current, i_p, is shown. Note that the current scale in (c) is 10× and in (d) is 100× that in (a) and (b).

6.3 Totally irreversible rxns.

B.C.2

$$\frac{i}{nFA} = D_o \left(\frac{\partial C_o(x,t)}{\partial t} \right)\Bigg|_{x=0} = k_f \, C_o(0,t)$$

$k_f = f(E)$

$$k_f = k_{f,i} \, e^{bt} = k_{f,i} \, e^{\alpha f v t}$$

E_i ; $k_{f,i} = k^0 \exp[-\alpha f(E_i - E^{0'})]$

$$i = nFAC_o^* (\pi D_o b)^{1/2} \chi(bt)$$

$$i_p = \alpha^{1/2} A \, C_o^* D_o^{1/2} v^{1/2} (\pi^{1/2} \chi)_{max}$$

0.4958

$(\phi(bt))_{max}$

$E_p = f(v)$

$\Rightarrow i_p$

$$\Rightarrow |E_p - E_{p/2}| = \frac{47.7}{\alpha} \text{ mV at } 25^\circ C$$

α ← kinetic parameters

Table 6.3.1
Current Functions $\sqrt{\pi}\chi(bt)$ for Irreversible Charge Transfer (3)[a,b]

Potential, mV	$\sqrt{\pi}\chi(bt)$	$\phi(bt)$	Potential, mV	$\sqrt{\pi}\chi(bt)$	$\phi(bt)$
160	0.003		15	0.437	0.323
140	0.008		10	0.462	0.396
120	0.016		5	0.480	0.482
110	0.024		0	0.492	0.600
100	0.035		−5	0.496	0.685
90	0.050		−5.34	0.4958	0.694
80	0.073	0.004	−10	0.493	0.755
70	0.104	0.010	−15	0.485	0.823
60	0.145	0.021	−20	0.472	0.895
50	0.199	0.042	−25	0.457	0.952
40	0.264	0.083	−30	0.441	0.992
35	0.300	0.115	−35	0.423	1.00
30	0.337	0.154	−40	0.406	
25	0.372	0.199	−50	0.374	
20	0.406	0.253	−70	0.323	

[a] The potential scale is $(E - E^{0\prime})\alpha n_a + (RT/F)\ln\sqrt{\pi D_O b}/k^0$.

[b] To calculate the current:

1. $i = i(\text{plane}) + i(\text{spherical correction})$.
2. $i = nFA\sqrt{bD_O}C_O^*\sqrt{\pi}\chi(bt) + nFAD_OC_O^*(1/r_0)\phi(bt)$.
3. $i = 602\, n(\alpha n_a)^{1/2}A\sqrt{D_O v}C_O^*[\sqrt{\pi}\chi(bt)] + 0.160(\sqrt{D_O}/r_0\sqrt{\alpha n_a v})\phi(bt)$ (at 25°).

Units for step 3 are the same as in Table 6.2.1.

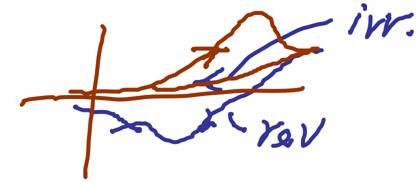

Dimensionless

$(\alpha F/RT)(E - E^{0\prime}) + \ln[(\pi D_O b)^{1/2}/k^0]$

$\alpha f v$

$E_p = f(\alpha, i, v)$

reversible

$E_p - E_{1/2}$

$\neq f(v)$ (steady state)

$E_p \neq f(v)$

6.4 Quasi-reversible Systems

(general solution)

B.C. 2

$$D_O \left(\frac{\partial C_O}{\partial x}\right)_{x=0} = k^0 e^{-\alpha f(E-E^{0'})} \left[C_O(0,t) - C_R(0,t) \cdot e^{f(E-E^{0'})} \right]$$

$$\Lambda = \frac{k^0}{(D_O^{1-\alpha} D_R^{\alpha} f v)^{1/2}}$$

Λ → ∞ → reversible

Λ → 0 irreversible

ψ(α, E)

if $D_O = D_R$

$$\Lambda = \frac{k^0}{(D f v)^{1/2}}$$

$$i = nFA D_O^{1/2} C_O^* f^{1/2} v^{1/2} \psi(E)$$

$$i_p = i_p(rev) \cdot K(\Lambda, \alpha)$$

O

CR

R

D → R

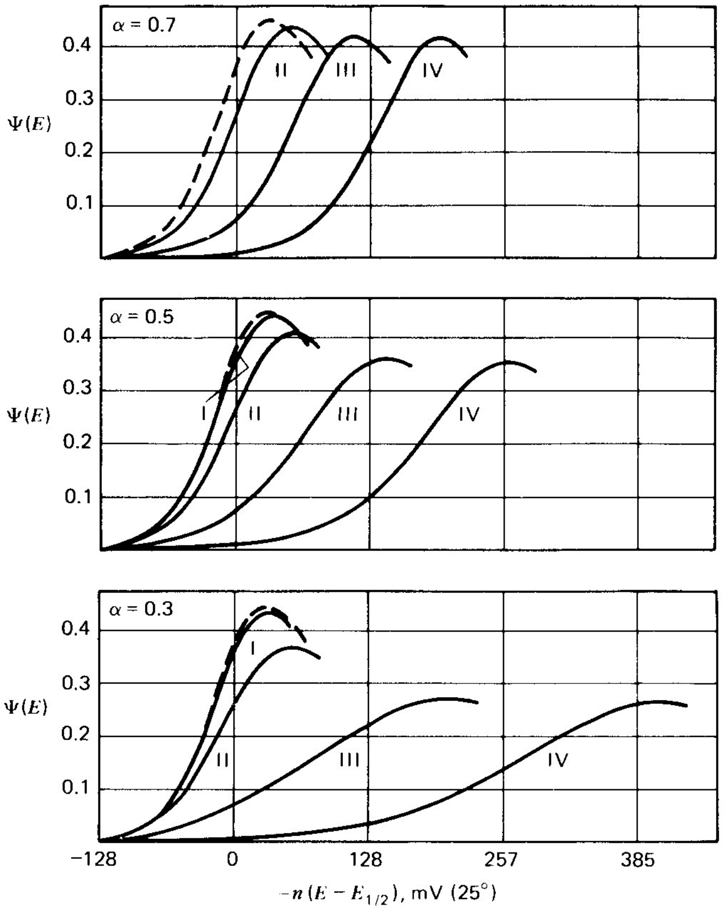

Figure 6.4.1

Variation of quasi-reversible current function, $\Psi(E)$, for different values of α (0.7, 0.5, 0.3, as indicated) and the following values of Λ: I, $\Lambda = 10$; II, $\Lambda = 1$; III, $\Lambda = 0.1$; IV, $\Lambda = 10^{-2}$. Dashed curve is for a reversible reaction.

$$\Psi(E) = i/nFAC_O^* D_O^{1/2}(nF/RT)^{1/2} v^{1/2}$$

$$\Lambda = k^0/D^{1/2}(nF/RT)^{1/2} v^{1/2} \qquad (\text{for } D_O = D_R = D)$$

[From H. Matsuda and Y. Ayabe, *Z. Elektrochem.*, **59**, 494 (1955), with permission.]

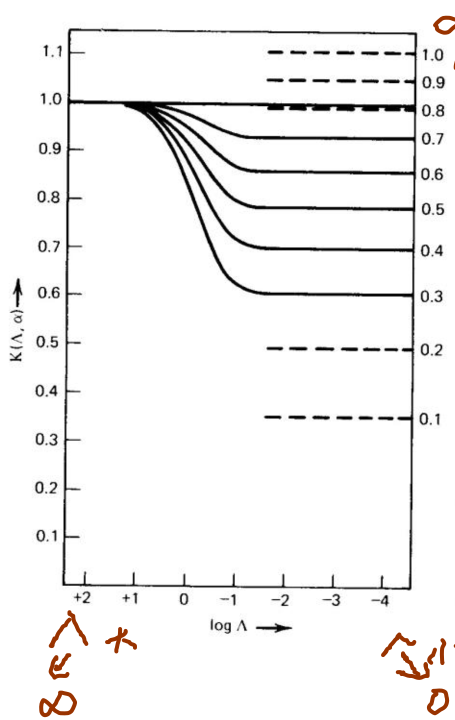

$i_p = i_p(rev) \cdot K(\Lambda, \alpha)$

Figure 6.4.2
Variation of $K(\Lambda, \alpha)$ with Λ for different values of α. Dashed lines show functions for totally irreversible reaction.

$$K(\Lambda, \alpha) = i_p/i_p(\text{rev})$$

[From H. Matsuda and Y. Ayabe, *Z. Electrochem.*, **59**, 494 (1955), with permission.]

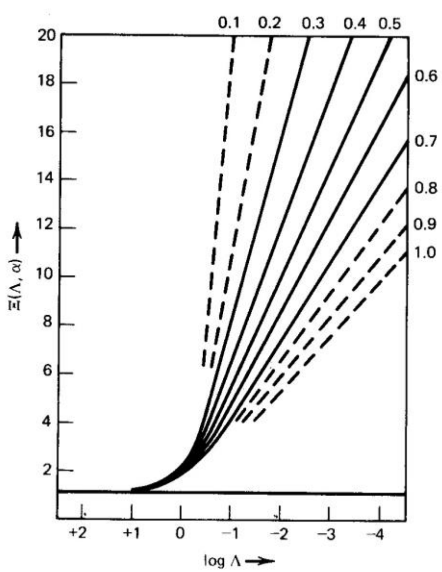

$E_{p/2} - E_p = \Delta(\Lambda, \alpha)\left(\frac{RT}{nF}\right)$

$= 26\,\Delta(\Lambda, \alpha)$ at 25°C

$E_p - E_{1/2} = -\frac{RT}{nF}\,\Xi(\Lambda, \alpha)$

Figure 6.4.3
Variation of $\Xi(\Lambda, \alpha)$ with Λ for different values of α. Dashed lines show functions for totally irreversible reaction.

$$\Xi(\Lambda, \alpha) = -(E_p - E_{1/2})\frac{nF}{RT}$$

[From H. Matsuda and Y. Ayabe, *Z. Elektrochem.*, **59**, 494 (1955), with permission.]

$\Lambda \geq 15$ ($k^0 \geq 0.3\,v^{1/2}$) reversible

$\Lambda \leq 10^{-2(1+\alpha)}$ ($k^0 \leq 2\times10^{-5}\,v^{1/2}$ cm/s) Totally irreversible

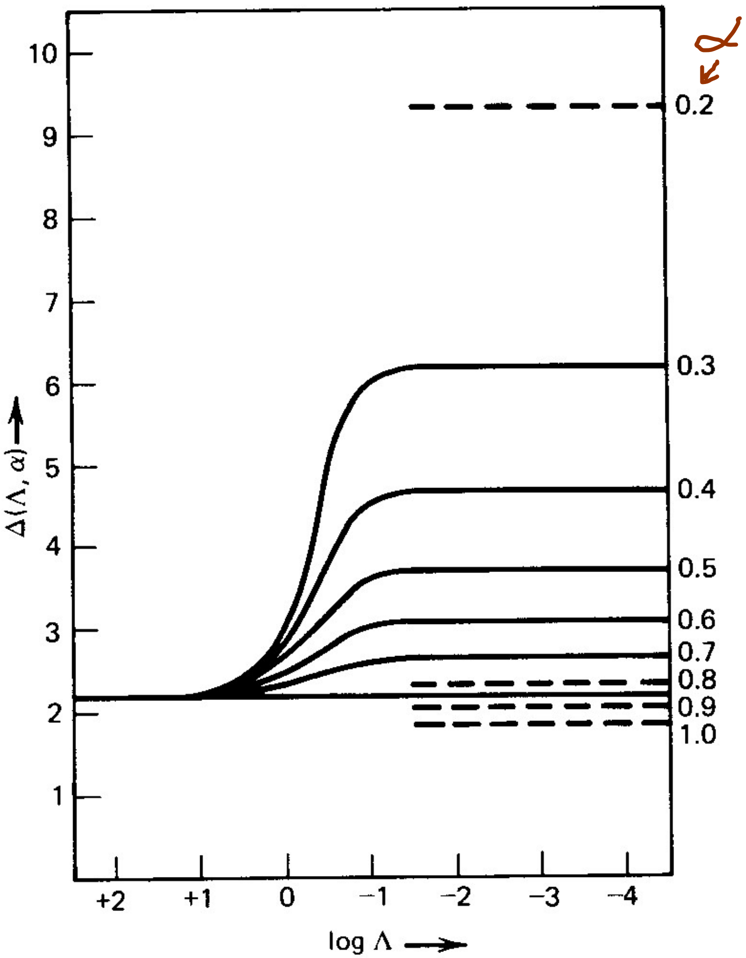

Figure 6.4.4

Variation of $\Delta(\Lambda, \alpha)$ with Λ and α. Dashed lines show values for totally irreversible reactions.

$$\Delta(\Lambda, \alpha) = (E_{p/2} - E_p)\,\frac{nF}{RT}$$

[From H. Matsuda and Y. Ayabe, *Z. Elektrochem.*, **59**, 494 (1955), with permission.]

6.5 CV

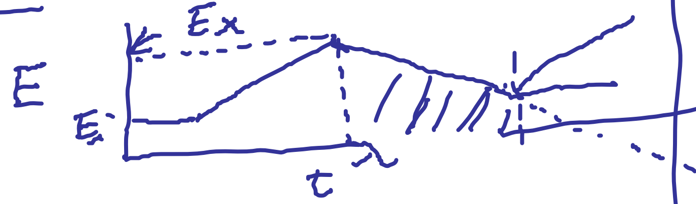

$0 \le t \le \lambda \quad E = E_i - vt$

$t \ge \lambda \quad E = (E_i - v\lambda) + v(t - \lambda)$

$= E_i - 2v\lambda + vt$

$S(t) = e^{\sigma t - 2\sigma\lambda}$

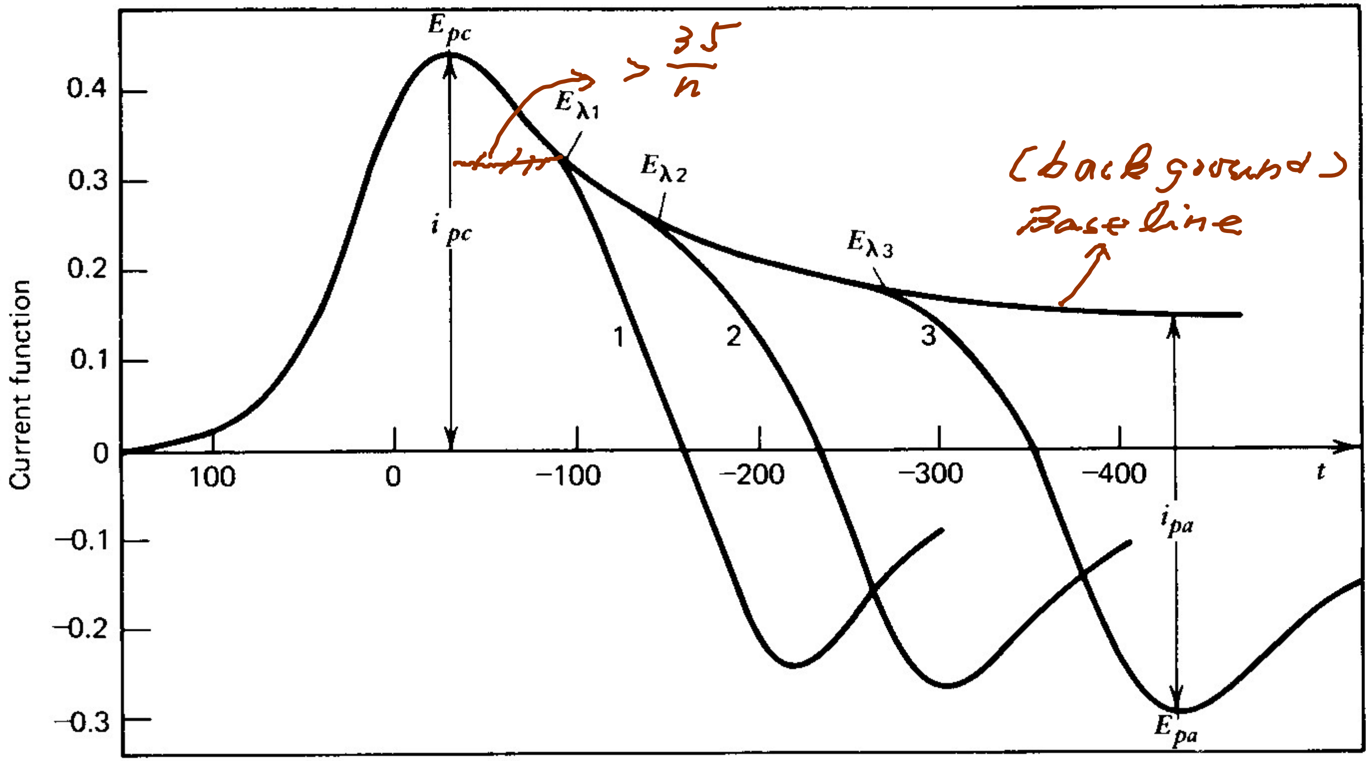

Figure 6.5.1

Cyclic voltammograms for reversal at different E_λ values with presentations as they appear on a strip-chart recorder (*i*-*t* curves).

$$\frac{i_{pa}}{i_{pc}} = \frac{(i_{pa})_0}{i_{pc}} + \frac{0.485(i_{sp})_0}{i_{pc}} + 0.086$$

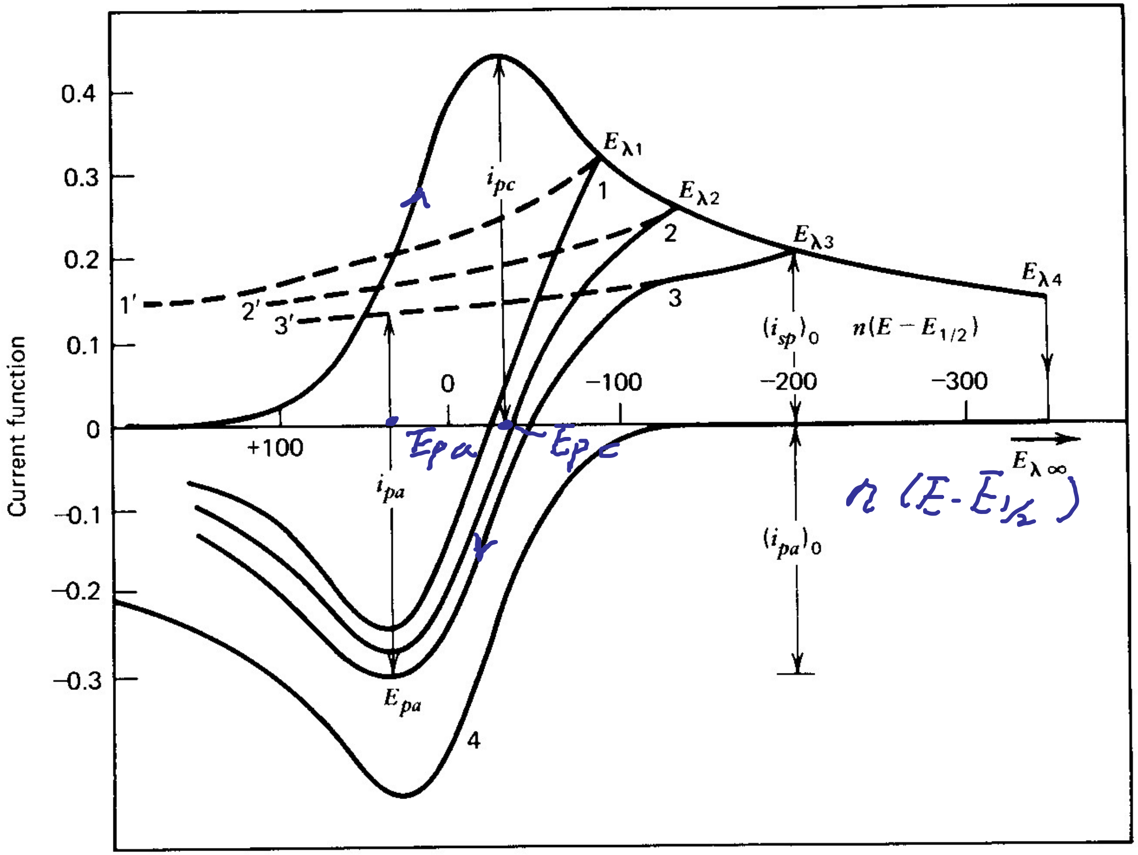

Figure 6.5.2

Cyclic voltammograms under the same conditions as in Figure 6.5.1 with presentations as they appear on X-Y recorder (*i-E* curves). E_λ of (1) $E_{1/2} - 90/n$; (2) $E_{1/2} - 130/n$; (3) $E_{1/2} - 200/n$ mV; (4) for potential held at $E_{\lambda 4}$ until the cathodic current decays to zero. [This curve results from reflection of the cathodic *i-E* curve through the *E* axis and then through the $n(E - E_{1/2}) = 0$ line. The curves in (1), (2), and (3) result by addition of this curve to the decaying current of the cathodic *i-E* curve.]

Table 6.5.1

Separation of Peak Potentials for a Nernstian Wave as a Function of E_λ[a]

$n(E_{pc} - E_\lambda)$ (mV)	$n(E_{pa} - E_{pc})$ (mV)
71.5	60.5
121.5	59.2
171.5	58.3
271.5	57.8
∞	57.0

[a] Adapted from Reference 3.

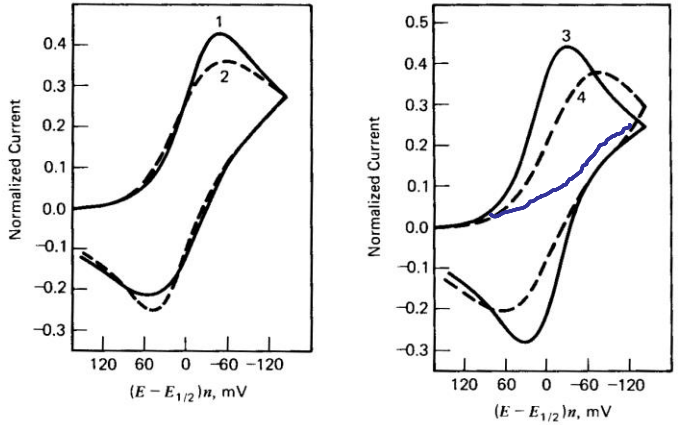

Figure 6.5.3

Theoretical cyclic voltammograms showing effect of ψ and α on curve shape. Curve 1: —— $\psi = 0.5$, $\alpha = 0.7$. Curve 2: $\cdots\cdot$ $\psi = 0.5$, $\alpha = 0.3$. Curve 3: —— $\psi = 7.0$, $\alpha = 0.5$. Curve 4: $\cdots\cdot$ $\psi = 0.25$, $\alpha = 0.5$. [Reprinted with permission from R. S. Nicholson, *Anal. Chem.*, **37**, 1351 (1965). Copyright 1965, American Chemical Society.]

Table 6.5.2
Variation of Peak Potential Separation (ΔE_p) with Kinetic Parameter ψ (9)[a]

ψ	$n(E_{pa} - E_{pc})$[b] mV
20	61
7	63
6	64
5	65
4	66
3	68
2	72
1	84
0.75	92
0.50	105
0.35	121
0.25	141
0.10	212

[a] For $E_\lambda = E_p - 112.5/n$ and $\alpha = 0.5$. ψ is defined in equation 6.5.5.
[b] $T = 25$ °C.

(reversible)

(irreversible)

6-6. Multiple components charge transfer rxns.

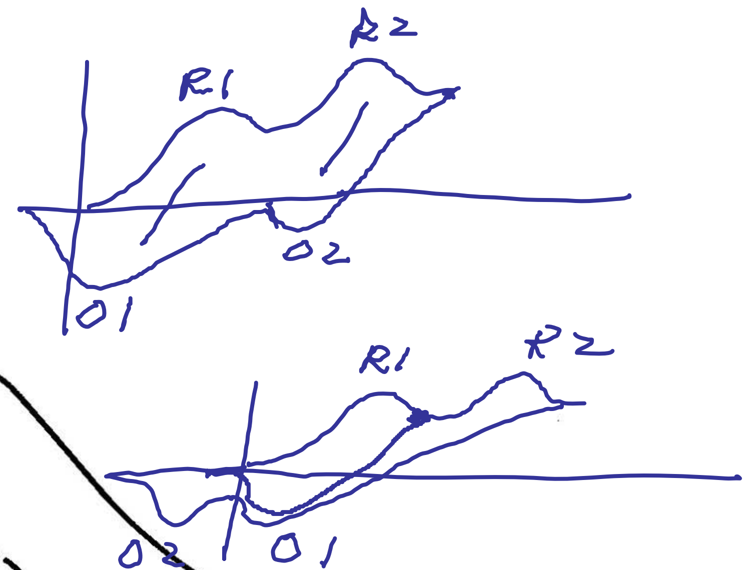

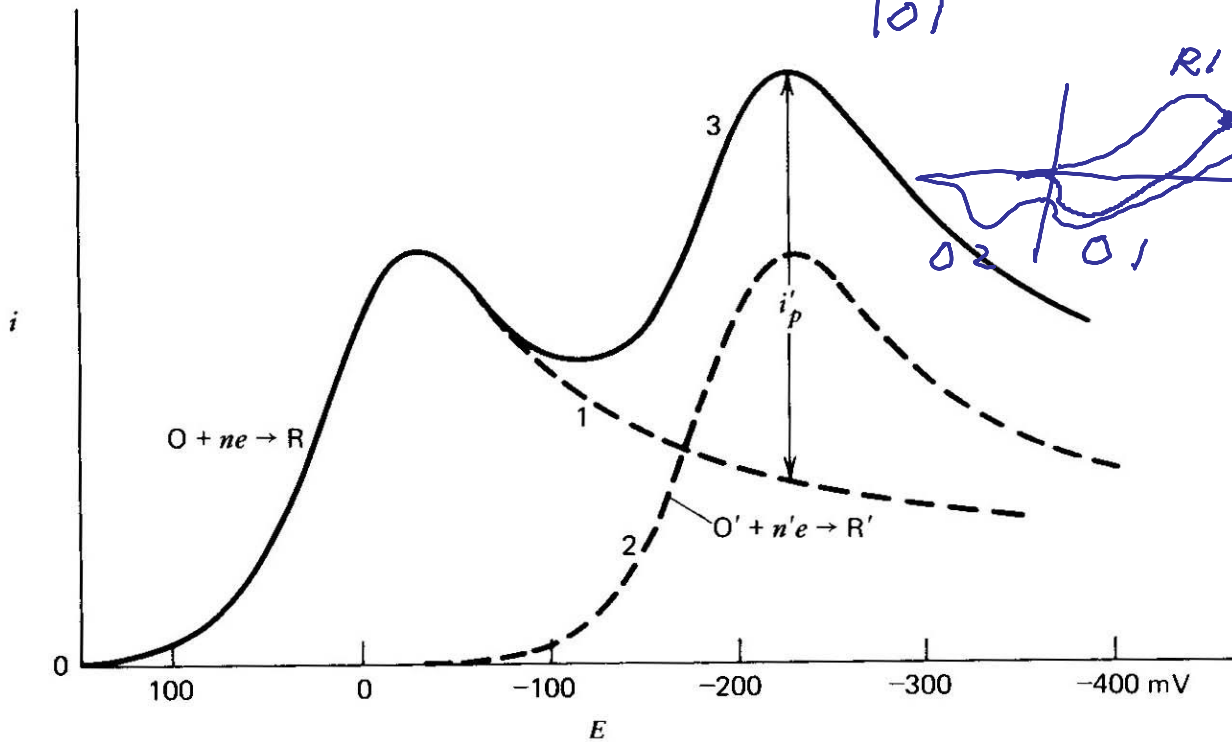

Figure 6.6.1
Voltammograms for solutions of (1) O alone; (2) O′ alone and, (3) mixture of O and O′, with $n = n'$, $C^*_O = C^*_{O'}$, and $D_O = D_{O'}$.

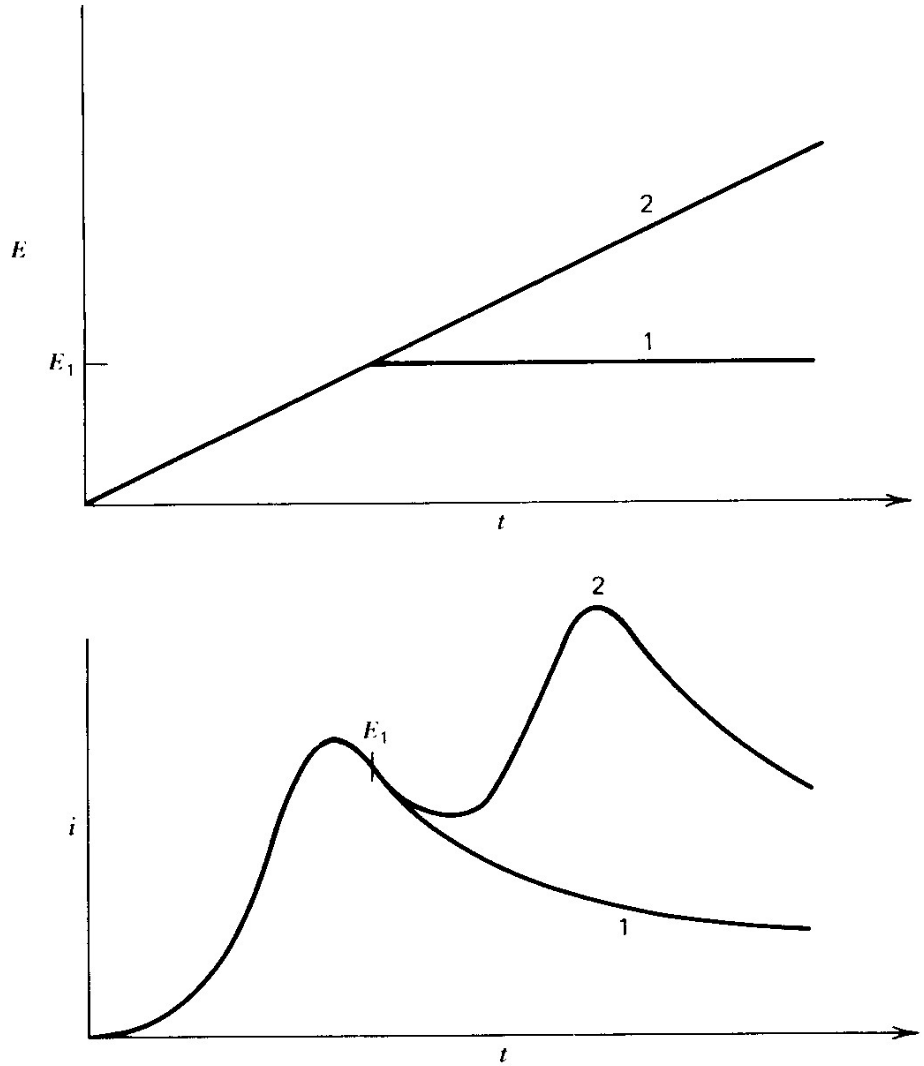

Figure 6.6.2

Method for obtaining baseline for measurement of i_p' of second wave. *Upper curves*: potential programs. *Lower curves*: resulting voltammograms with curve 1 potential stopped at E_1, curve 2 potential scan continued. System as in Figure 6.6.1.

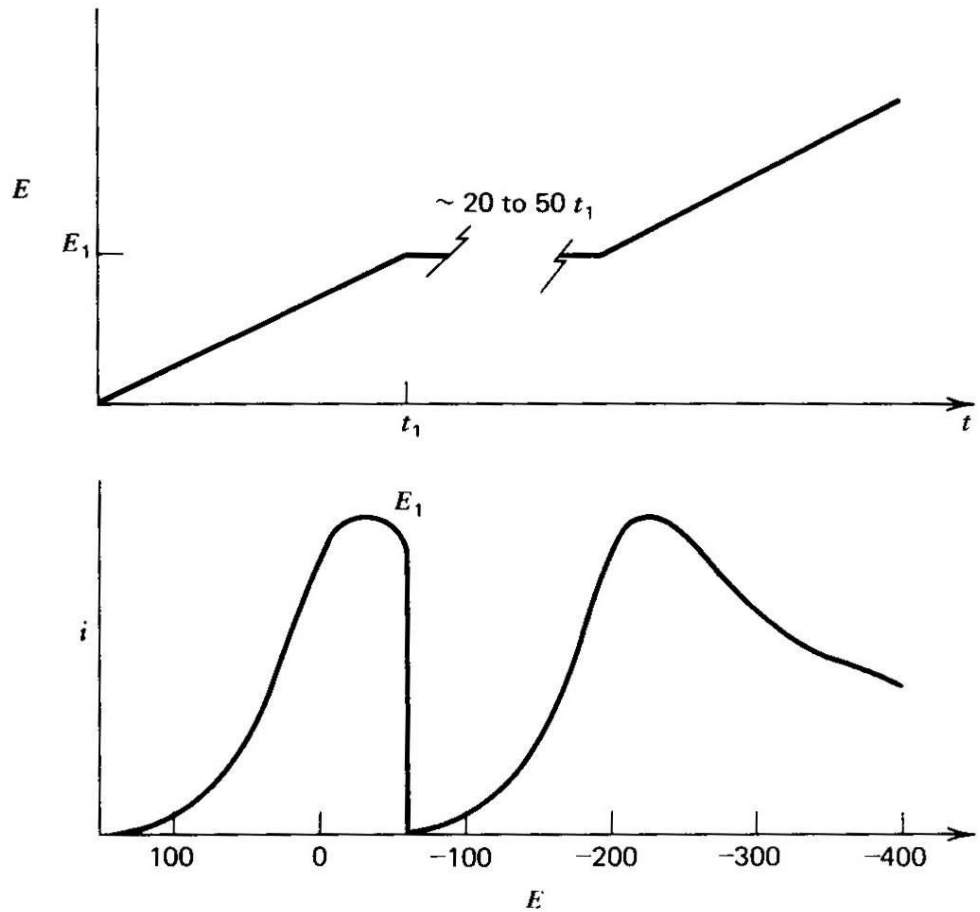

Figure 6.6.3
Method of allowing current of first wave to decay before scanning second wave. *Upper curve*: potential program. *Lower curve*: resulting voltammogram. System as in Figure 6.6.1.

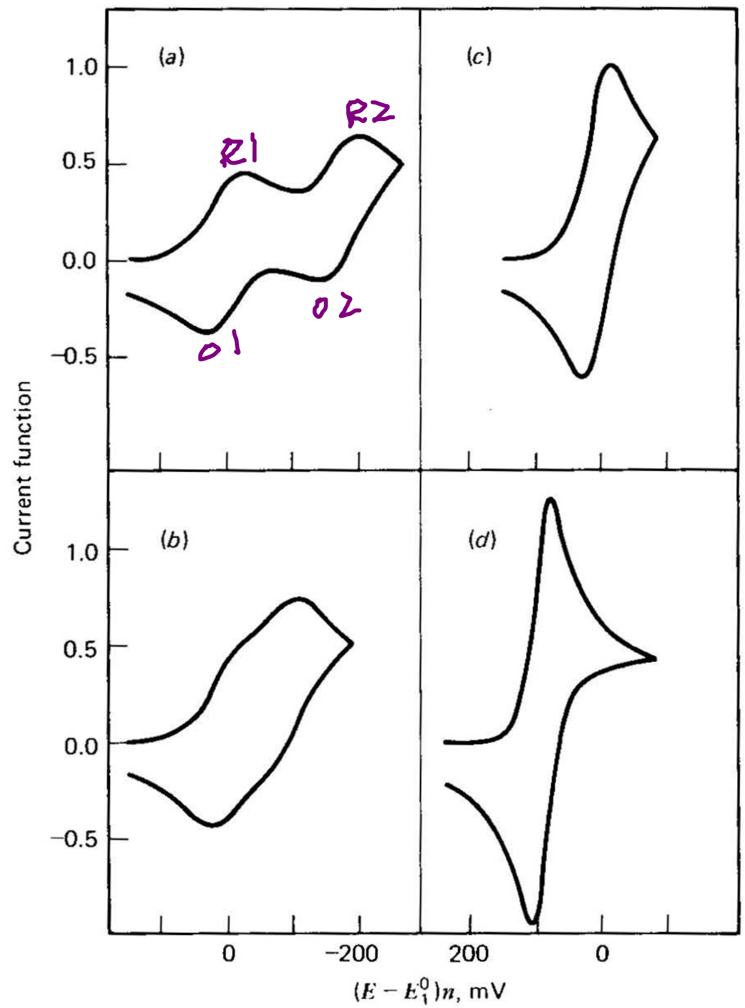

Figure 6.6.4

Cyclic voltammograms for a reversible two-step system. Current function is analogous to $\chi(z)$ defined in (6.2.16). $n_2/n_1 = 1.0$. (*a*) $\Delta E^0 = -180$ mV. (*b*) $\Delta E^0 = -90$ mV. (*c*) $\Delta E^0 = 0$ mV. (*d*) $\Delta E^0 = 180$ mV. [Reprinted with permission from D. S. Polcyn and I. Shain, *Anal. Chem.*, **38**, 370 (1966). Copyright 1966, American Chemical Society.]

$O + ne = R$ (1) E_1^0

$O' + n'e = R'$ (2) E_2^0

$\Delta E^0 = E_2^0 - E_1^0$

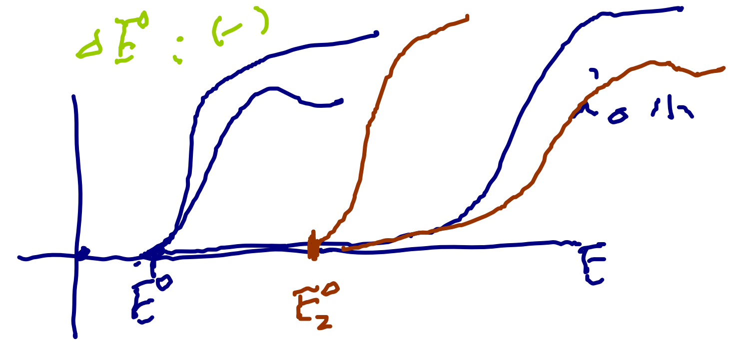

$O + ne = R_1$ E_1^0

$R_1 + n'e = R_2$ E_2^0

O adsorbed on electrode

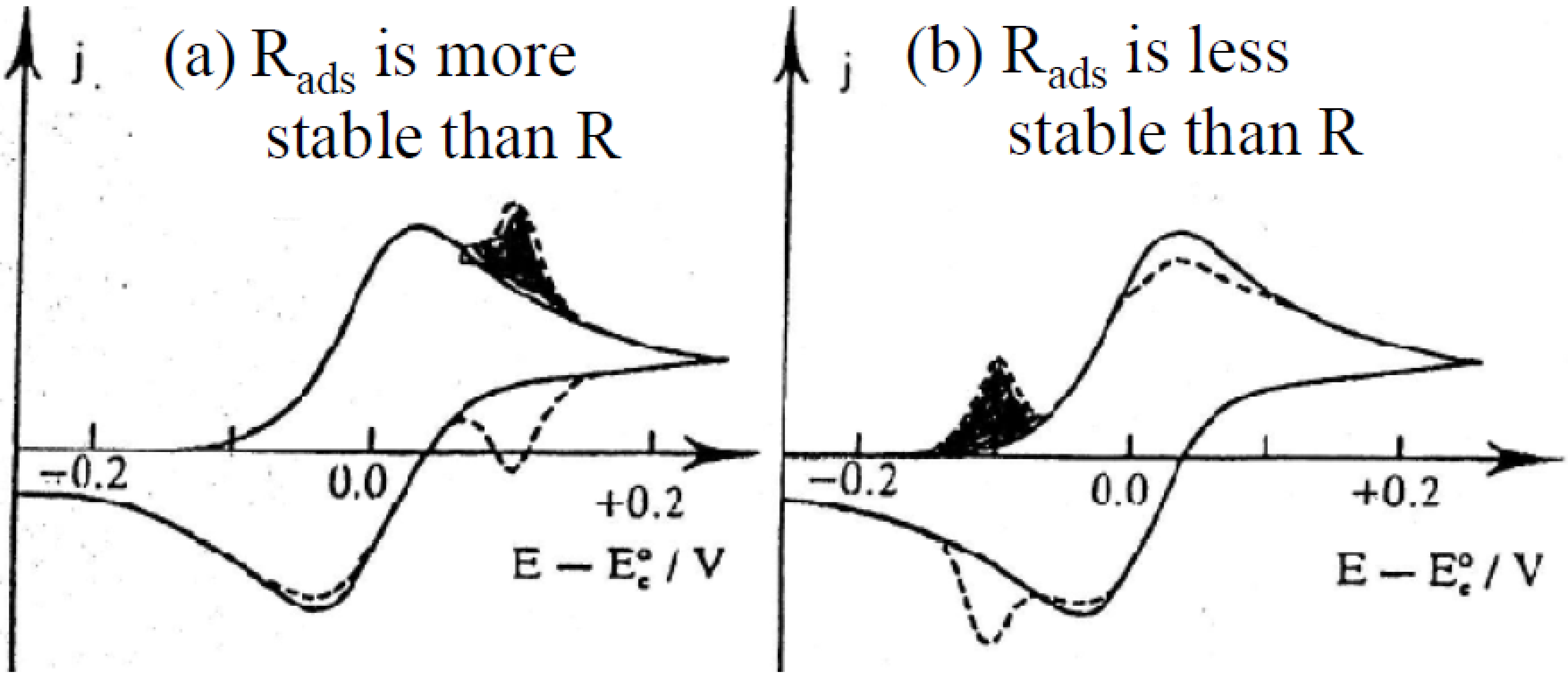

Phase formation

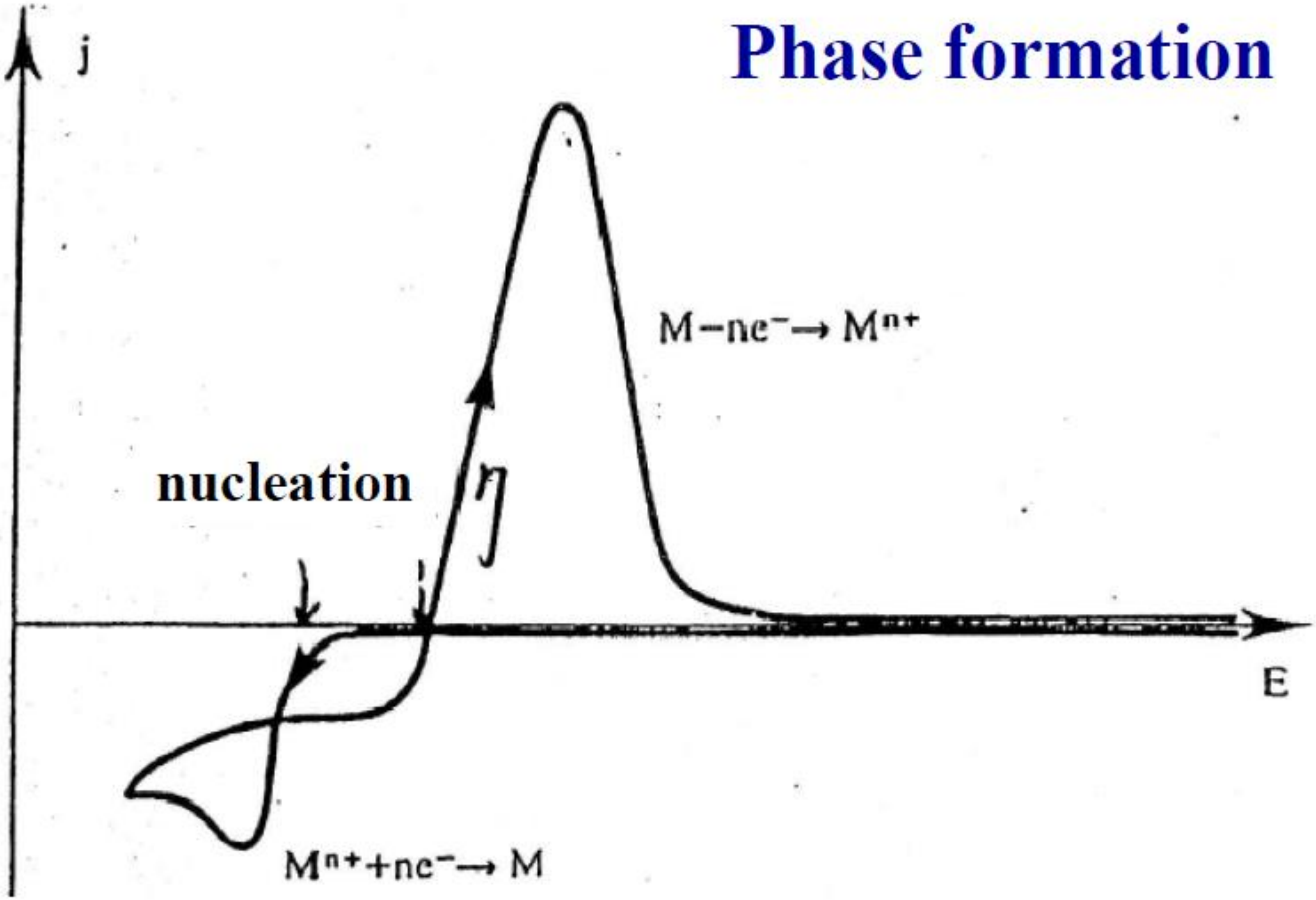

$R_{ads} - ne^- \rightleftharpoons O$

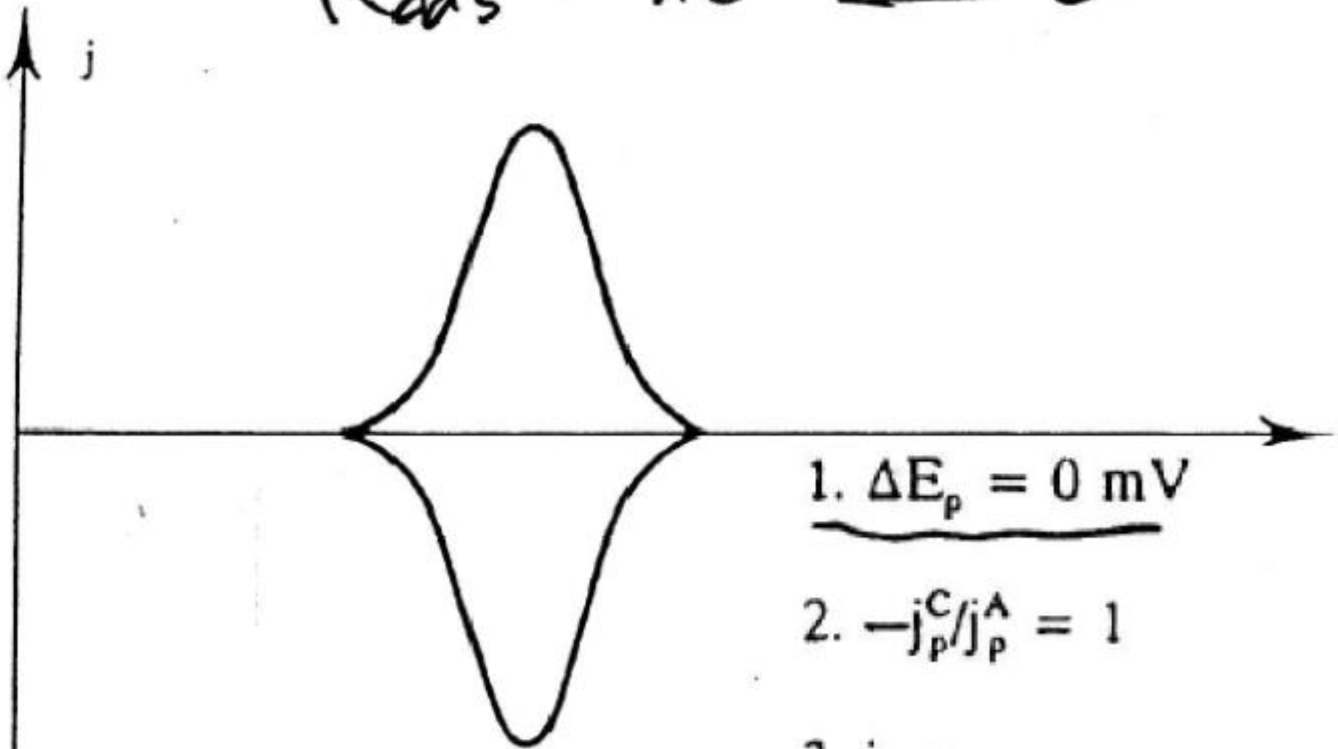

1. $\Delta E_p = 0$ mV
2. $-j_p^C / j_p^A = 1$
3. $j_p \propto \nu$
4. E_p are independent of ν
5. $q_A = q_C \leq q_{monolayer}$

RDE

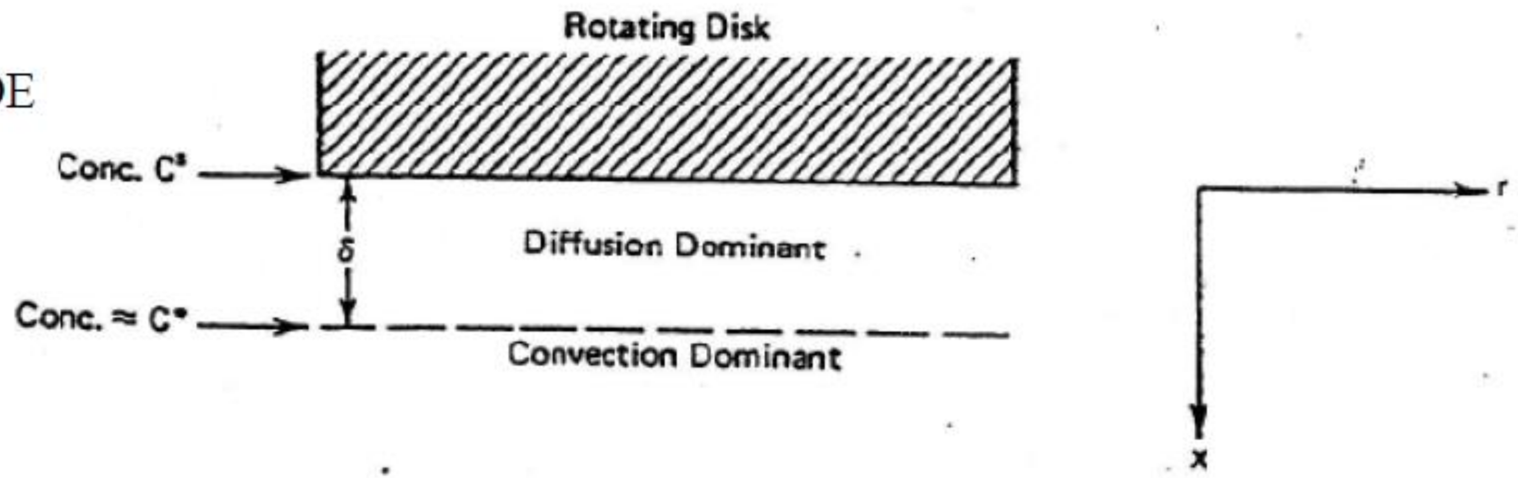

Figure 11-3. Model for convective diffusion.

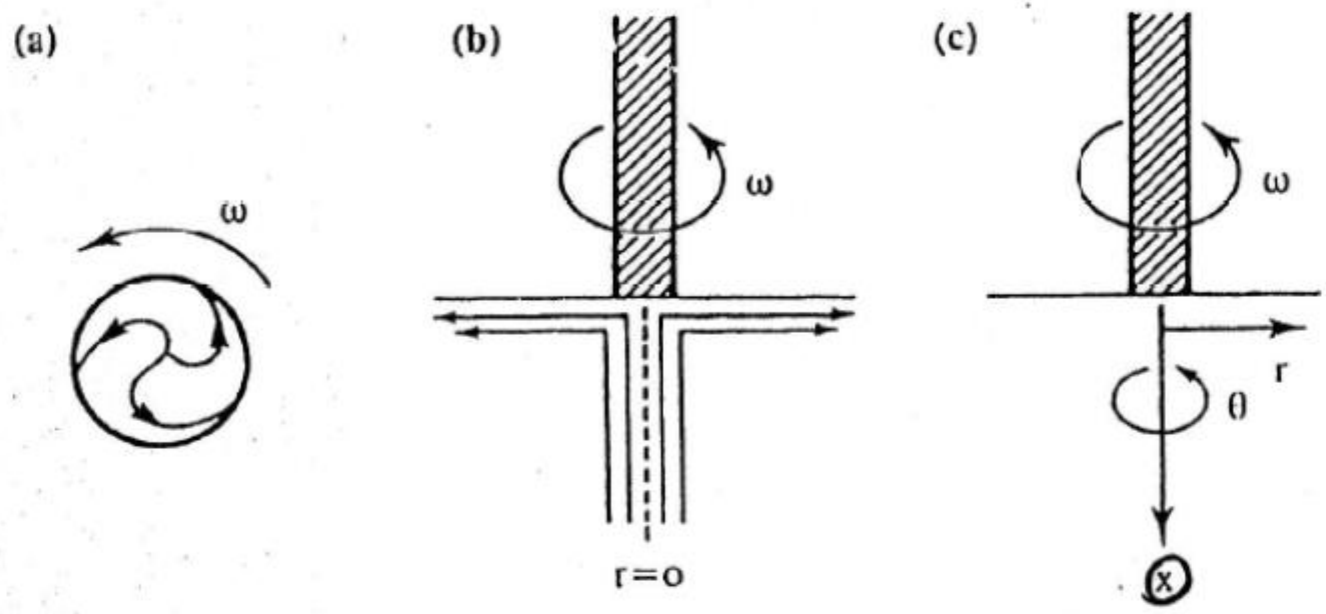

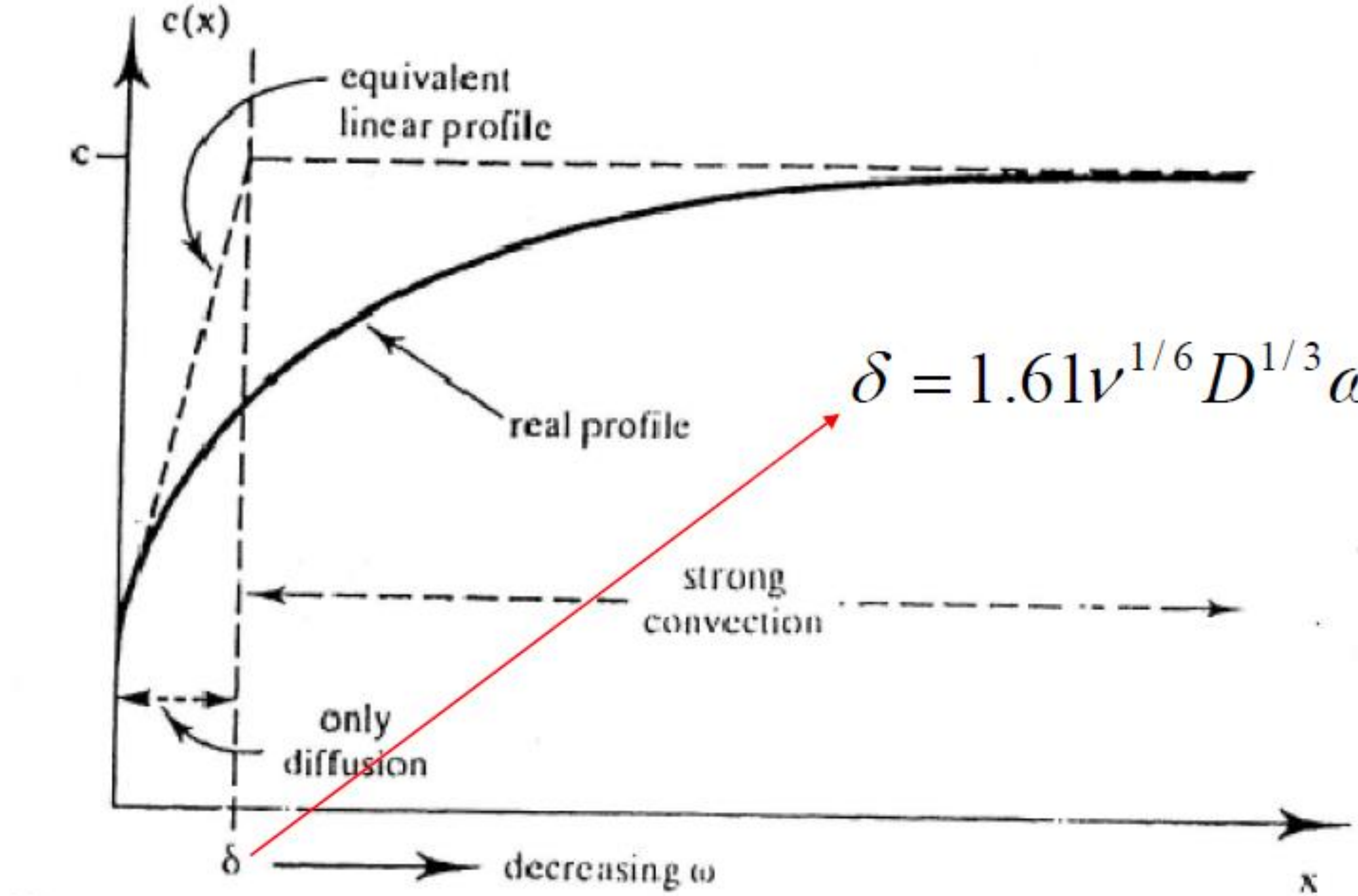

$$\delta = 1.61\nu^{1/6} D^{1/3} \omega^{-1/2}$$

Figure 6.7 *Concentration profile for the electroactive species using the concept of a Nernst boundary layer.*

$$i_L = nFD\left(\frac{dC}{dx}\right)_{x=0} = nFD\frac{C}{\delta}$$

$$= 0.62nFD^{2/3}C\nu^{-1/6}\omega^{1/2} \qquad (Levich \quad eqn.)$$

C = solution concentration, mol/cm^3

i_L = limiting current, A

ν = kinematic viscosity of the fluid, cm^2/s

ω = angular velocity of the disk (ω = 2πN, N = rps)

Koutecky-Levich plots

$$\frac{1}{I} = \frac{1}{nFAk_{et}C} + \frac{1.61\nu^{1/6}}{nFACD^{2/3}}\frac{1}{\omega^{1/2}}$$

As $\omega \rightarrow \infty, \Rightarrow \qquad \frac{1}{I} = \frac{1}{nFAk_{et}C}$

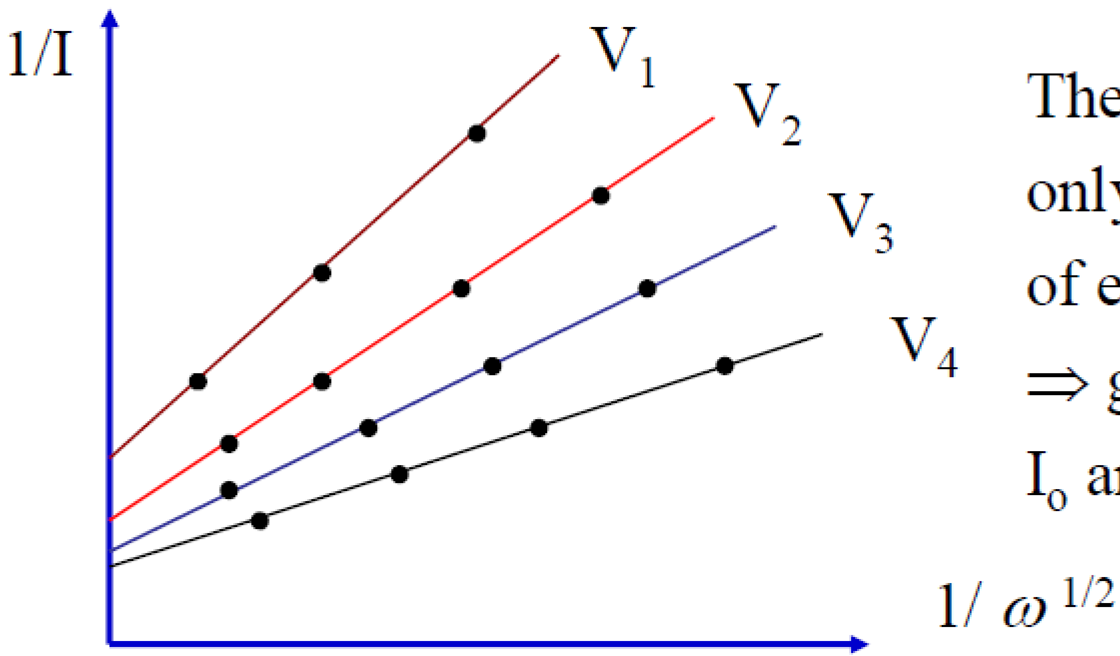

The intercept of *y* (i.e., 1/I) is only dependent upon the rate of electron transfer (i.e., E) $\Rightarrow$ get the Tafel plot to obtain I_o and α

The RRDE

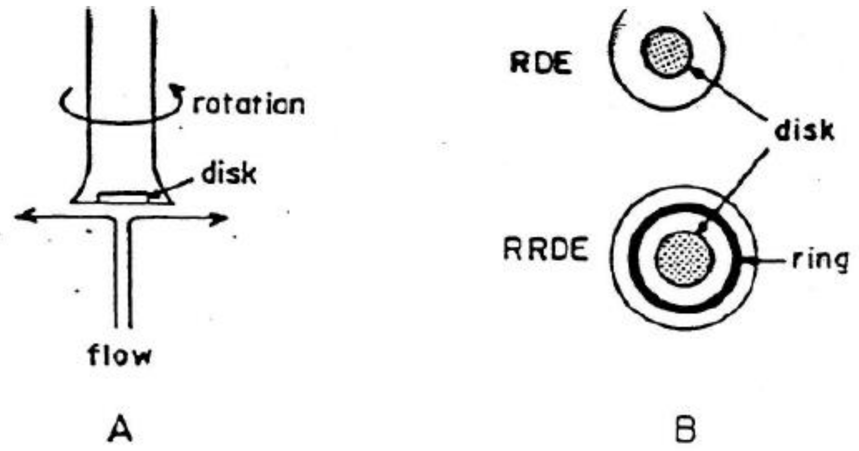

Figure 3.39 (A) Rotating-disk electrode with hydrodynamic flow pattern. (B) Bottom view of rotating-disk electrode (RDE) and rotating ring-disk electrode (RRDE).

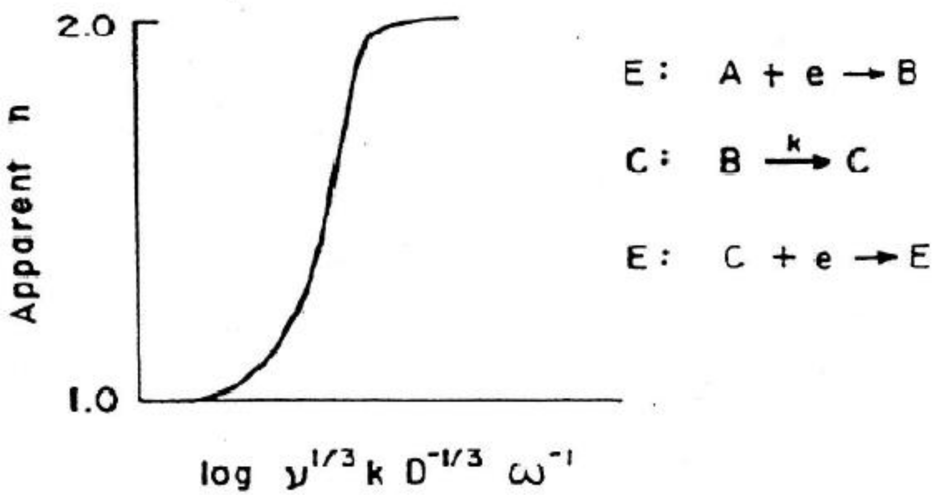

Figure 3.40 Variation in "apparent n" as a function of angular velocity of an RDE for the ECE mechanism.

The ORR on RRDE

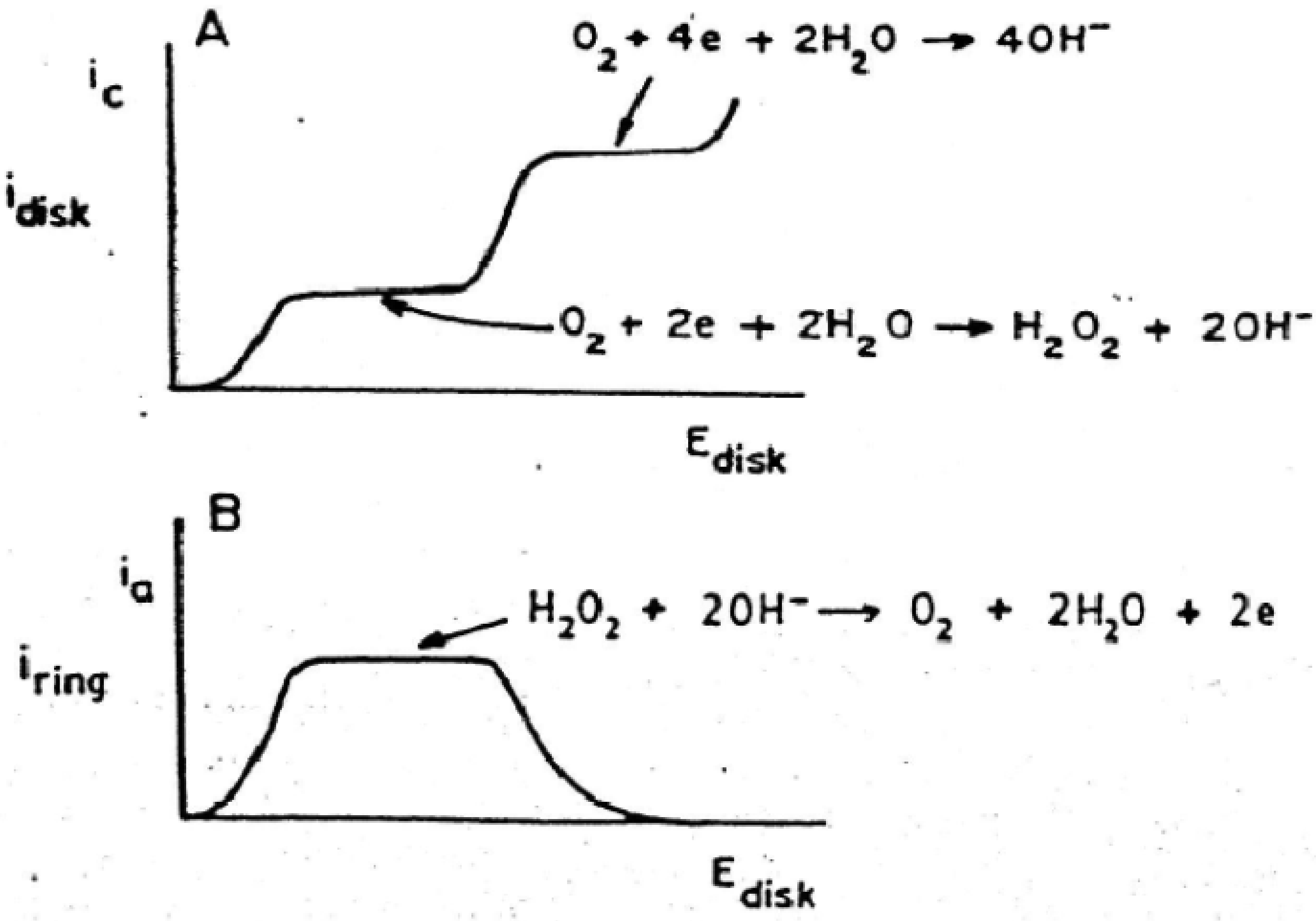

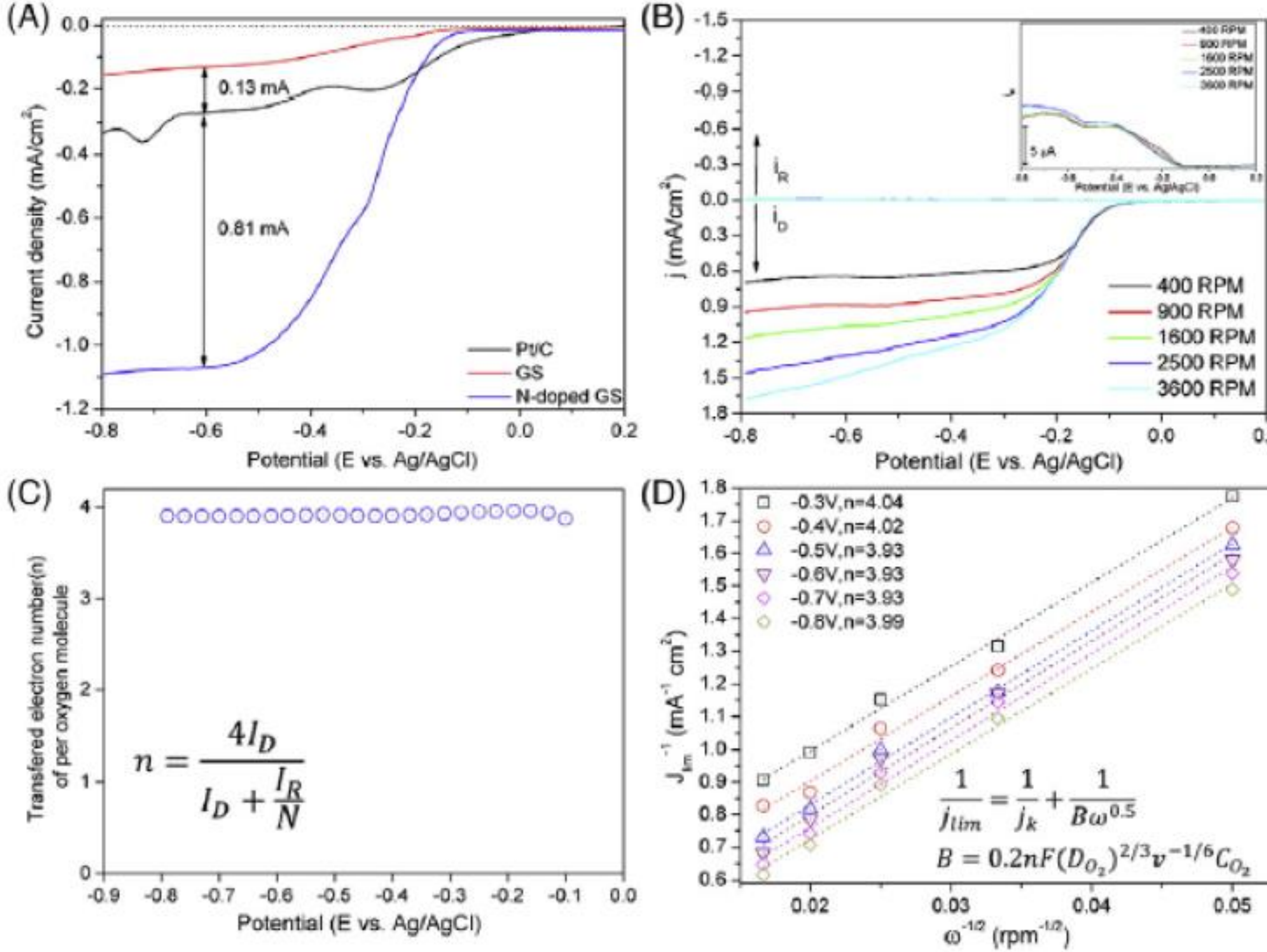

(A)
Current density (mA/cm^2)
Potential (E vs. Ag/AgCl)
0.13 mA
0.81 mA
Pt/C
GS
N-doped GS
(B)
j (mA/cm^2)
Potential (E vs. Ag/AgCl)
i_R
i_D
400 RPM
900 RPM
1600 RPM
2500 RPM
3600 RPM
5 μA
(C)
Transfered electron number(n) of per oxygen molecule
Potential (E vs. Ag/AgCl)
$n = \frac{4I_D}{I_D + \frac{I_R}{N}}$
(D)
-0.3V,n=4.04
-0.4V,n=4.02
-0.5V,n=3.93
-0.6V,n=3.93
-0.7V,n=3.93
-0.8V,n=3.99
J_{lim}^{-1} (mA^{-1} cm^2)
$\omega^{-1/2}$ (rpm$^{-1/2}$)
$\frac{1}{j_{lim}} = \frac{1}{j_k} + \frac{1}{B\omega^{0.5}}$
$B = 0.2nF(D_{O_2})^{2/3}v^{-1/6}C_{O_2}$

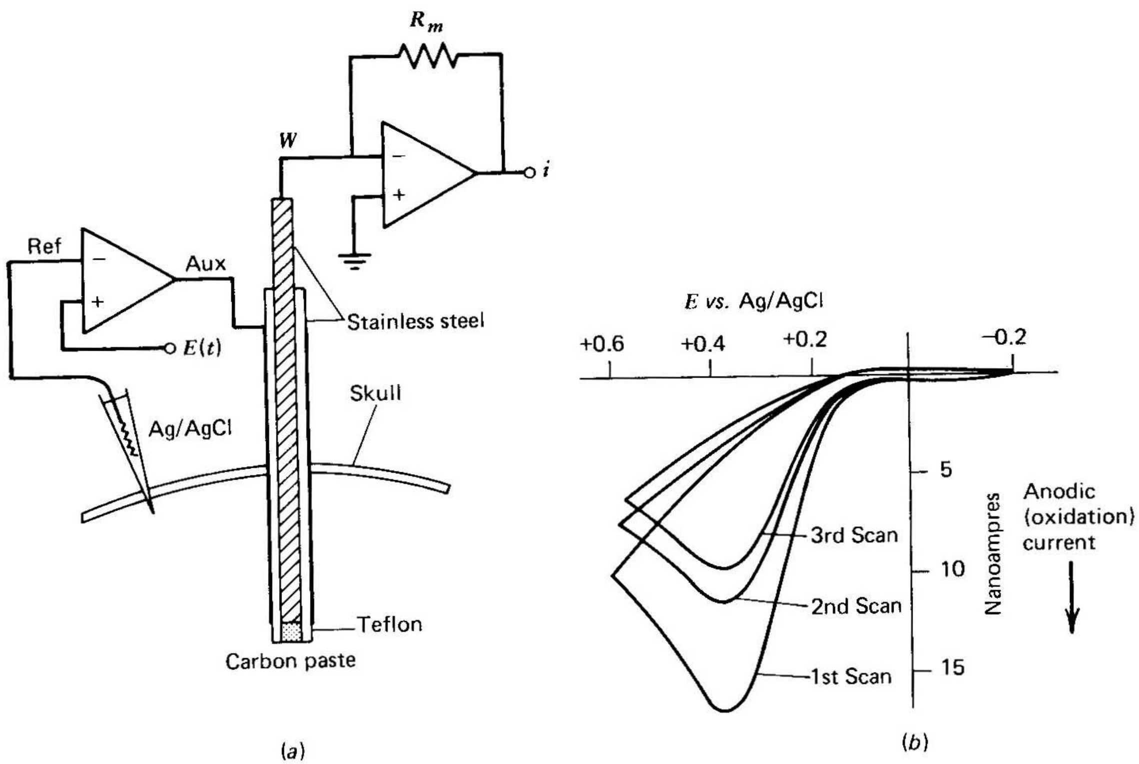

Figure 6.6.5

Application of cyclic voltammetry to in vivo analysis in brain tissue. (*a*) Carbon paste working electrode, stainless steel auxiliary electrode (18-gauge cannula), Ag/AgCl reference electrode, and other apparatus for voltammetric measurements. (*b*) Cyclic voltammogram for ascorbic acid oxidation at C-paste electrode positioned in the caudate nucleus of an anesthetized rat. [From P. T. Kissinger, J. B. Hart, and R. N. Adams, *Brain Res.*, **55**, 20 (1973), with permission.]